CERAMIC MEMBRANES I

Edited by

H.U. Anderson
A. C. Khandkar
M. Liu

Phase Related Oxygen Permeation Through Sr-Doped $LaCoO_{3-\delta}$

René H.E. van Doorn, Henny J.M. Bouwmeester and Anthonie J. Burggraaf.

University of Twente, Laboratory of Inorganic Materials Science, P.O. Box 217, 7500 AE Enschede, the Netherlands.

Abstract

Oxygen permeation results through $La_{1-x}Sr_xCoO_{3-\delta}$ are reported. It is shown that in the temperature region 750 - 775 °C an order-disorder of the oxygen sublattice occurs. The low temperature ordered phase is studied by X-Ray powder diffraction (XRD), neutron diffraction as well as selected area electron diffraction (SAED) together with High Resolution Transmission Electron Microscopy (HRTEM) coupled with Parallel Electron Energy Loss Spectroscopy (PEELS) and Energy Dispersive X-Ray spectroscopy (EDX). Although the long range methods XRD and neutron diffraction showed no indications for an oxygen vacancy ordering, SAED and HRTEM showed micro domains exhibiting an $a_c \times a_c \times 2a_c$ superstructure, along with regions without indications for a superstructure. The superstructure could be interpreted in terms of an oxygen vacancy ordering due to which a large part of the oxygen vacancies were trapped in regions with the superstructure and so effectively reducing the ionic conductivity. By means of PEELS it was shown that the cobalt ions within the superstructure regions have a higher oxidation state than the cobalt ions in the non-ordered regions.

1. Introduction

Perovskite type of materials (ABO_3), of which the ideal structure is given in Fig. 1, attract a fair amount of interest for oxygen separation applications. The perfect centrosymetric cubic symmetry (Spacegroup $Pm\bar{3}m$) allows all six oxygen ions to contribute equally to the oxygen vacancy transport, via a hopping mechanism, through these materials. Besides this ability to transport oxygen vacancies through the material, a second prerequisite for application of these materials for oxygen separation membranes is the presence of electronic conductivity [1]. It is by now well known that the lanthanide transition metals based perovskites fulfil both requests. By acceptor doping these lanthanide transition metal perovskites oxygen vacancies can be created, which increase the ionic conductivity further. It is further well known that the degree of reducibility of the transition metal ion positively correlates with the ionic conductivity.

Initial work by Teraoka *et al.* [2] and later by van Doorn *et al.* [1,3] have shown that the oxygen flux through membranes made out of Sr-doped $LaCoO_3$ (LSC) are among the highest known in literature. Van Doorn *et al.* [1,3] showed that the oxygen flux through 2 mm thick samples LSC is for doping levels up to 60% primarily determined by the ionic conductivity. It was shown by Kruidhof *et al.* [4] that oxygen vacancy ordering within perovskites might negatively influence the ionic conductivity. By means of high temperature ^{17}O-NMR Adler *et al.* [5] showed that LSC doped with 20 atom% Cu on the Co site shows a disordering around 800 °C on which all available oxygen ions become mobile. Recent Mott-Littleton computer simulations by Cherry *et al.* [6] have shown that the oxygen ion diffusion through $LaCoO_{3-\delta}$ indeed occurs via a hopping mechanism. The pathway of

diffusion is, however, not along the expected <110> edge of the CoO_6 octahedron but shows a slight convex curvature.

2. Theory

The bulk diffusion limited oxygen transport through a dense mixed conducting membrane placed in an oxygen gradient can be described by Wagner's theory of oxide film growth [7]:

$$j_{O_2} = \frac{RT}{4^2 F^2 L_{Mem}} \int_{a''_{O_2}}^{a'_{O_2}} t_{ion}\, t_{el}\, \sigma_{total}\, d\ln a_{O_2} \qquad (1)$$

Here j_{O_2} stands for the oxygen permeation flux (mol cm^{-2} s^{-1}), L_{mem} the membrane thickness (cm), t_{ion} and t_{el} for the ionic and electronic transference number of the total conductivity (S cm^{-1}) respectively. The boundaries of integration are the oxygen activities at the high pressure side (denoted by a single prime) and at the lower partial pressure side (denoted by a double prime), other symbols have there usual meaning. For LSC the ionic conductivity is several orders of magnitude lower than the electronic ($t_{el} \approx 1.0$) [8], so the oxygen transport is rate limited by the ionic conductivity. This reduces eq. (1) to:

$$j_{O_2} = \frac{RT}{4^2 F^2 L_{Mem}} \int_{a''_{O_2}}^{a'_{O_2}} \sigma_{ion}\, d\ln a_{O_2} \qquad (2)$$

Since the ionic conductivity is primarily anionic, the ionic conductivity is given by the following simple Nernst-Einstein relation:

$$\sigma_{ion} = \frac{c_I z_I^2 D_I F^2}{RT} \qquad (3)$$

where c_I is the molar concentration of oxygen anions with valence charge z_I (= -2) and D_I the oxygen self-diffusion coefficient (cm^2 s^{-1}). For a simple vacancy diffusion mechanism, D_I is related to the vacancy diffusion coefficient (D_V, cm^2 s^{-1}) by:

$$c_V D_V = c_I D_I \qquad (4)$$

with c_V the molar concentration of oxygen vacancies. Assuming high screening of the oxygen vacancies and ideal behaviour, c_V is equal to δ/V_M with δ the non-stoichiometry parameter and V_M the perovskite molar volume (cm^3). So the oxygen flux through a bulk diffusion limited membrane is given by, where the oxygen activities have been replaced by oxygen partial pressures:

$$j_{O_2} = \frac{D_V \delta^o}{4nL_{Mem} V_M}\left(p'^n_{O_2} - p''^n_{O_2}\right) \qquad (5)$$

In case that the screening of the oxygen vacancies is not optimal (interaction between the oxygen vacancies), the δ/V_M-value for c_V has to be replaced by $\alpha\,\delta/V_M$ in which α is the fraction of the oxygen vacancies which are mobile and contributing to the hopping of the oxygen vacancies and hence to the ionic conductivity. In the derivation of eq. (5) an isotropic D_V has been assumed. For a non cubic (super)structure this might not necessarily be true and preferential diffusion paths in one or more directions might exist, such as the *a,b*-plane for $YBa_2Cu_3O_{6+\delta}$. For multicrystalline samples, such as used in this study, this preferential paths will cancel out by increasing the diffusion path and thus introducing a tortuosity factor as also known in the transport theory through porous membranes.

3. Experimental

Compositions LSC with Sr contents x=0.2-0.7 were made by thermal decomposition of metal-EDTA complexes as explained in more detail elsewhere [9]. Powders were calcined at temperatures 850 - 900 °C. After calcination powders were ball milled for 2 hours at 55 - 60 rpm using YSZ balls

and a polyethylene container. Disks of 20.0 mm were made by uniaxial pressing at 1.5 MPa followed by isostatic pressing at 400 MPa and sintering at 1100 - 1200 °C under stagnant air. From the thus obtained rods (density 95+% of theoretical) membranes of diameter 12.0 mm and thickness 0.5 - 2.0 mm were cut and polished with SiC (1000 MESH). These membranes were used for oxygen permeation using a quartz reactor. Details of which can be found elsewhere [10].

Phase purity and lattice parameters were determined by powder XRD on the powders after calcination at 900 °C [11,12]. Samples of composition x=0.5 and 0.7 were also analysed by High Resolution Transmission Electron Microscopy (HRTEM) and Selected Area Electron Diffraction (SAED). Using either a Philips CM30 TWIN/(S)TEM fitted with a double tilt goniometer stage (± 45°) at 300 keV and an aperture of 0.1 - 0.2 μm (point resolution 2.3 Å) or a Philips CM30ST FEG fitted with a double stage goniometer stage (± 20°) at 300 keV, the latter being operated at the national centre for High Resolution Transmission Electron Microscopy (Delft, the Netherlands, resolution 1.3 Å). Measurements were performed at both liquid nitrogen as well as ambient temperature. Aselect chosen regions of the samples were analysed by means of EDX (LINK using the CM30ST FEG) and Parallel Electron Energy Loss Spectroscopy (PEELS) using the CM30 and a Gatan Model 666 analyser with Gatan Software version 2.11. PEELS measurements were carried out at liquid nitrogen temperature to prevent the formation of a C-layer during the measurements. For Co/O ratios the peak locations were calibrated against the zero loss peak, using an energy setting of 0.5 eV per channel and the Co-$L_{2,3}$ and the O-K-peak. For exact location of the Co-$L_{2,3}$-peaks an energy dispersion of 0.2 eV per channel was used with reference to the La-$M_{4,5}$-peaks. Before analyses were carried out, samples were gently pestled and ultrasonically dispersed in ethanol followed by deposition on carbon coated copper grids. A sample with composition x=0.7 annealed under air at 650 °C for 15 hours was studied by neutron diffraction using a vanadium sample holder on the High-Flux Reactor of the ECN in Petten (The Netherlands). A wavelength of 2.5718 Å was used. Data collection was performed at room temperature from 15 to 155° (2θ) in steps of 0.1° (2θ). Pyloric graphite (thickness 120 mm) was used as a second-order filter and Soller slits with a horizontal divergence of 0.5° were placed before the monochromator and in front of the four ^{3}He counters. A 42 × 24 mm^2 diaphragm has been used. Data analysis was performed using the Rietveld Method with the 1991 release of DBWS-9006 assuming Gausian peak shapes. DTA experiments were performed on powdered samples, using a Setaram TG DTA92 with heating and cooling rates of 10 °C min^{-1}.

4. Results

In a previous study [3] it was already shown that the oxygen permeation flux through a 2.0 mm thick membranes of doping levels of less than 70% is bulk limited, so by studying the oxygen permeation through these compositions one basically studies the ionic conductivity of a compound. The Arrheniusplot for the oxygen permeation through a 2.0 mm thick sample of $La_{0.5}Sr_{0.5}CoO_{3-\delta}$ under an air *vs* 10 ml(STP) He min^{-1} gradient is shown in Fig. 2. A small but measurable anomaly is observed in the temperature region 750 - 775 °C. Similar anomalies were observed for compositions x = 0.4 - 0.7 as far as studied [3]. Below 750 °C (so below the anomaly temperature) long stabilisation times before steady state was reached were observed. On cooling from higher temperatures the permeation rate dropped considerably during these stabilisation times (see Fig. 3). Once the steady state was reached, a further decrease in temperature again led to long stabilisation times. Heating the sample above 750 °C normally resulted in fast equilibration times of the order of 1 h and less. During these stabilisations, an increase of the flux was observed [1]. Although the exact temperature was shifted to a somewhat higher temperatures (*viz.* 790 °C) similar observations were made by Kruidhof *et al.* [4] for $SrCo_{0.8}Fe_{0.2}O_{3-\delta}$. These authors attributed the observed phenomena to the occurrence of an order-disorder transition within the oxygen sublattice and the progressive growth of micro domains of an ordered phase.

The DTA curves for $La_{1-x}Sr_xCoO_{3-\delta}$ under air showed a small endothermic heat effect after which the slope of the signal significantly increased. Associated with this endothermic heat effect a small

weight loss in the TGA signal was observed. So there are clear indications that a phase transition, most probably associated with a small change in the oxygen non-stoichiometry, occurs in these materials.

Only for $La_{0.3}Sr_{0.7}CoO_{3-\delta}$ small indications for a possible superstructure could be observed in the XRD-pattern (see the peaks at 2θ-values 23.3°, 25.3° and 28.2° in Fig. 4). All other doping levels showed no indications by XRD. Since XRD is a rather long range technique and also not too sensitive for lighter elements such as oxygen, this not necessary means that no superstructure is present in the other compositions. The neutron powder diffraction spectrum of a sample $La_{0.3}Sr_{0.7}CoO_{3-\delta}$ annealed under air at 650 °C for 15 h and subsequently furnace cooled could be indexed on basis of a cubic perovskite using spacegroup $Pm\bar{3}m$ without any indications for a superstructure. The absence of superstructure indications in this neutron diffraction spectrum, whereas the XRD spectrum of the same sample showed indications for a superstructure is explained by the too small size of the regions exhibiting a superstructure to be observed by neutron diffraction (≤ 2000 Å). Refinement of the oxygen site occupancy showed a value of 0.94±0.003 (δ=0.18±0.01). SAED patterns of the same powder (see Fig. 5) showed a doubling of one of the unit cell axis at a time, indicating an $a_c \times a_c \times 2a_c$ superstructure. Apart from the regions exhibiting the mentioned indications for a superstructure, regions exhibiting only reflections due to the cubic perovskite were also observed. HRTEM pictures of the same region (shown in Fig. 6) showed micro domains with a width of 500 Å and smaller exhibiting a linestructure parallel along one of the unit cell axis, also indicating an $a_c \times a_c \times 2a_c$ superstructure.

So although the long range methods XRD and neutron powder diffraction didnot give strong indications for a superstructure, SAED as well HRTEM clearly show that there are regions exhibiting a superstructure with doubling along the unit cell axis.

(P)EELS measurements in regions exhibiting a superstructure showed the same La as well as Sr concentration as regions without a superstructure. The Co/O ratios were, however, increased for regions with a superstructure as compared with regions without a superstructure. These results strongly suggest that the superstructure is due to ordering within the oxygen sublattice, contrary to the results of Gai and Rao on $La_{0.5}Sr_{0.5}CoO_{3-\delta}$, who suggested an ordering within the cation A-site lattice [13]. On basis of these results we propose the superstructure shown in Fig. 7. The superstructure is described by a tetragonal $A_2B_2O_5$ structure in which two anti-facing square pyramids are present. Thus resulting in two different oxygen sites; one at the apex of the pyramid and four in the basal plane of the pyramid. A more detailed description of the superstructure will be presented elsewhere [14].

Experiments to obtain the high temperature phase by annealing powder at temperatures above 750 °C (up to 1200 °C), followed by either furnace cooling or quenching in ice water, all failed as indicated by the presence of superstructure reflections in SAED. This is attributed to a high driving force for ordering.

Co belongs to the first row transition metals with a $3d^6$ electron configuration for Co^{3+} and a $3d^5$ configuration for Co^{4+}. From ligand field (crystal field stabilisation) theory it is well known that ions exhibiting a $3d^5$ electron configuration show a preference for a square pyramidal co-ordination, whereas ions with a $3d^6$ electron configuration show a preference for octahedral co-ordination. From these considerations, an ordering of Co^{3+}/Co^{4+} over ordered and non-ordered regions might be expected. PEELS measurements with an energy setting of 0.2 eV channel^{-1} showed a small shift (0.8 eV) to higher energy losses for the Co in a superstructure region as compared with Co in non superstructure regions as is shown in Fig. 8. The fact that only 0.8 eV difference is found in stead of the 17.8 eV on basis of the difference between ionisation potentials is explained by the high iternitant electronic conductivity exhibited by these materials, allowing for an effective screening. Nonetheless the ordering results in a trapping of the vacancies (see eq. (6)) and is thus reducing the ionic conductivity of the material as compared with the ideal perovskite with random distribution of the oxygen vacancies.

$$\left(Co_{Co}^{\cdot} - V_O^{\cdot\cdot} - Co_{Co}^{\cdot}\right) \rightleftarrows 2Co_{Co}^{\cdot} + V_O^{\cdot\cdot} \qquad (6)$$

Recent ^{17}O-NMR results by Adler *et al.* [5] and Russek [15] on LSC with 20 atom% Cu B-site doping indicate that the similar local ordering observed in those materials disappears around 800 °C, as indicated by the increased number of mobile oxygen vacancies. Preliminary ^{17}O-NMR on LSC tend to indicate that the same holds for the LSC materials. It should here, however, be noted that ^{17}O-NMR measurements only probe the mobile oxygen ions with its surrounding and as such give only very indirect information on the local surrounding (structure) of the materials. To gain such information, ^{59}Co or ^{127}La-NMR experiments should be performed at high temperature. Due to the ferroelectromagnetism present in LSC, such measurements are very difficult to perform and to the best of our knowledge no information in literature is present on high temperature NMR of the given elements within LSC. Oxygen non-stoichiometry measurements performed by Lankhorst *et al.* [16] on $La_{0.8}Sr_{0.2}CoO_{3-\delta}$ above 800 °C indicate, however, that the oxygen vacancies are completely disordered.

5. Conclusions

It is shown that although XRD and neutron diffraction show no (clear) indications for a superstructure in LSC, an $a_c \times a_c \times 2a_c$ type oxygen vacancy ordered superstructure at temperatures below 750-775 °C is present. Due to this ordering, oxygen vacancies are trapped and cannot contribute to the ionic conductivity and hence effectively reduce the oxygen permeation transport through these materials. Above 775 °C a randomly disordered perovskite is formed. ^{17}O-NMR results indicate that there are an increased number of oxygen ions present above this temperature, which also explains the increased permeation flux observed in LSC above 775 °C.

Acknowledgements

The help of Ing. H. Kruidhof in performing part of the oxygen permeation experiments is gratefully mentioned. Dr. E. G. Keim and Dr. T. Kachlicki are acknowledged for their help with HRTEM as well as PEELS measurements.

Literature cited

[1] R.H.E. van Doorn, H. Kruidhof, H.J.M. Bouwmeester and A.J. Burggraaf, "Oxygen Permeation through Sr-Doped $LaCoO_{3-\delta}$ Perovskites," *Proc. MRS Fall Meeting 1994 Boston* (1994).

[2] Y. Teraoka, H.-M. Zhang, S. Furukawa and N. Yamazoe, "Oxygen Permeation Through Perovskite-Type Oxides," *Chem. Lett.*, 1743 - 46 (1985).

[3] R. H. E. van Doorn, H. Kruidhof, H. J. M. Bouwmeester and A. J. Burggraaf, "Oxygen Permeation Through Dense Ceramic Membranes of Sr-Doped $LaCoO_{3-\delta}$ Perovskites," *Submitted to J. Electrochem Soc.* (1995).

[4] H. Kruidhof, H.J.M. Bouwmeester, R.H.E. van Doorn and A.J. Burggraaf, "Influence of Order-Disorder Transitions on Oxygen Permeability Through Selected Nonstoichiometric Perovskite-Type Oxides," *Solid State Ionics*, **63 - 65**, 816 - 22 (1993).

[5] S. Adler, S. Russek, J. Reimer, M. Fendorf, A. Stacy, Q. Huang, A. Santoro, J. Lynn, J. Baltisberger and U. Werner, "Local Structure and Oxide-Ion Motion in Defective Perovskites," *Solid State Ionics*, **68[3&4]**, 193 - 211 (1994).

[6] M. Cherry, M.S. Islam and C.R. Carlow, "Oxygen Ion Migration in Perovskite-type Oxides," *J. Solid State Chem.*, in press (1995).

[7] C. Wagner, "Beitrag zur Theorie des Anlaufsvorgangs," *Z. Phys. Chem,* **B21,** 25 - 41 (1933). (German).
[8] J. Mizusaki, J. Tabuchi, T. Matsuura, S. Yamauchi and K. Fueki, "Electrical Conductivity and Seebeck Coefficient of Nonstoichiometric $La_{1-x}Sr_xCoO_{3-\delta}$," *J. Electrochem. Soc,* **136[7],** 2082 - 88 (1989).
[9] R.H.E. van Doorn, H. Kruidhof, A.J.A. Winnubst, H.J.M. Bouwmeester and A.J. Burggraaf, "Preparation of Perovskite Ceramics by Decomposition of Metal-EDTA Complexes," *Submitted to J. Amer. Ceram. Soc.* (1995)
[10] H.J.M. Bouwmeester, H. Kruidhof, A.J. Burggraaf and P.J. Gellings, "Oxygen Semipermeability of Erbia-stabilized Bismuth Oxide," *Solid State Ionics,* **53 - 56,** 460 (1992).
[11] R.H.E. van Doorn, J. Boeijsma, and A.J. Burggraaf, "Powder diffraction of $La_{0.3}Sr_{0.7}CoO_{3-\delta}$," Powder Diffraction, **9[3],**
[12] N.M.L.N.P. Closset, R.H.E. van Doorn, H. Kruidhof and J. Boeijsma, "The Crystal Structure of $La_{1-x}Sr_xCoO_{3-\delta}$ ($0 \leq x \leq 0.6$)", Powder Diffraction, *in press.*
[13] P.L. Gai and C.N.R. Rao, "Cation Ordering in $Ln_{1-x}Sr_xCoO_3$," *Mat. Res. Bull.,* **10,** 787 - 90 (1975).
[14] R.H.E. van Doorn, E.G. Keim, T. Kachlicki, H.J.M. Bouwmeester and A.J. Burggraaf, "Oxygen Vacancy Ordering in Sr-Doped $LaCoO_{3-\delta}$ Perovskites," *To be published* (1995).
[15] S.L. Russek, "Air Separation with Perovskite-type Oxide Membranes Membrane Materials Considerations," *Thesis UC at Berkeley* (1993).
[16] M.H.R. Lankhorst, H.J.M. Bouwmeester, B.A. Boukamp and H. Verweij, "Oxygen Non-Stoichiometry and Oxygen Diffusivity of Mixed Conducting Perovskites," *This conference.*

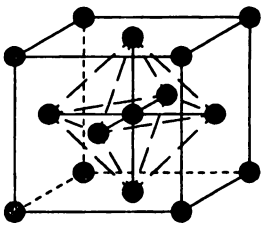

Fig. 1 Ideal cubic perovskite lattice.

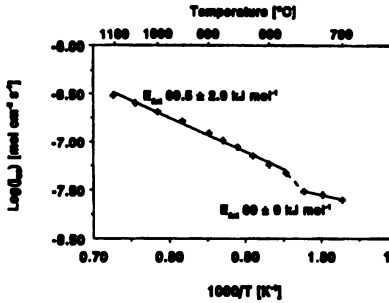

Fig. 2 Arrheniusplot of the oxygen permeatio for $La_{0.5}Sr_{0.5}CoO_{3-\delta}$

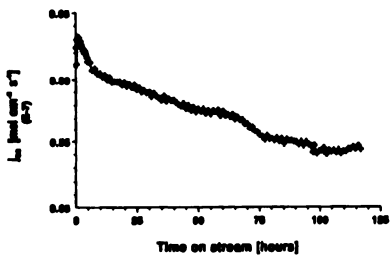

Fig. 3 Steady state transitions for $La_{0.5}Sr_{0.5}CoO_{3-\delta}$

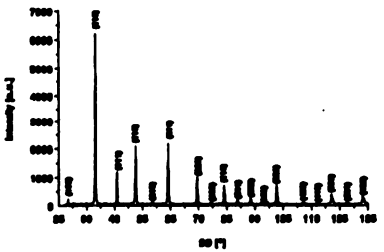

Fig. 4 XRD spectrum of $La_{0.5}Sr_{0.7}CoO_{3-\delta}$.

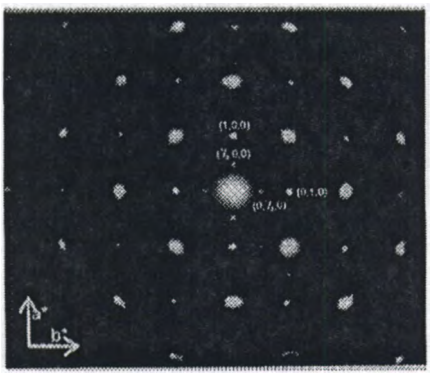

Fig. 5 SAED pattern of $La_{0.5}Sr_{0.7}CoO_{3-\delta}$ aligned along the c-axis.*

Fig. 6 HRTEM picture of $La_{0.5}Sr_{0.7}CoO_{3-\delta}$ superstructure region.

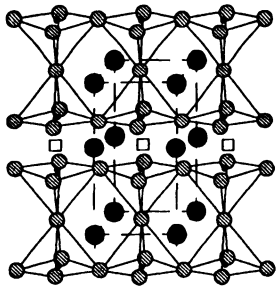

Fig. 7 Proposed superstructure.

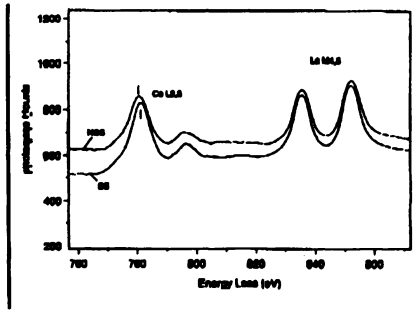

Fig. 8 PEELS signal for regions with superstructure (SS) and without (NSS).